Cell Death and Differentiation (2011) 18, 1161–1173

www.nature.com/cdd

Diacylglycerol kinase α regulates the formation and polarisation of mature multivesicular bodies involved in the secretion of Fas ligand-containing exosomes in T lymphocytes

R Alonso[1,5], C Mazzeo[2,5], MC Rodriguez[1], M Marsh[3], A Fraile-Ramos[4], V Calvo[2], A Avila-Flores[4], I Merida[4] and M Izquierdo*[,2]

Multivesicular bodies (MVBs) are endocytic compartments that contain intraluminal vesicles formed by inward budding from the limiting membrane of endosomes. In T lymphocytes, these vesicles contain pro-apoptotic Fas ligand (FasL), which may be secreted as 'lethal exosomes' upon fusion of MVBs with the plasma membrane. Diacylglycerol kinase α (DGKα) regulate the secretion of exosomes, but it is unclear how this control is mediated. T-lymphocyte activation increases the number of MVBs that contain FasL. DGKα is recruited to MVBs and to exosomes in which it has a double function. DGKα kinase activity exerts a negative role in the formation of mature MVBs, as we demonstrate by the use of an inhibitor. Downmodulation of DGKα protein resulted in inhibition of both the polarisation of MVBs towards immune synapse and exosome secretion. The subcellular location of DGKα together with its complex role in the formation and polarised traffic of MVBs support the notion that DGKα is a key regulator of the polarised secretion of exosomes.
Cell Death and Differentiation (2011) **18,** 1161–1173; doi:10.1038/cdd.2010.184; published online 21 January 2011

Exosomes are small-membrane vesicles of endocytic origin that are secreted by many cells. These vesicles are formed by inward budding of the limiting membrane of late endosomes, and accumulate as intraluminal vesicles (ILVs) inside multivesicular bodies (MVBs).[1] Stimulation of cells induces the fusion of the limiting membrane of the MVBs with the plasma membrane (PM) and the secretion of the ILVs, which then are termed as exosomes.[1]

Cytotoxic T lymphocytes (CTLs) use both perforin/granzyme and Fas ligand (FasL)-dependent pathways to exert their function. Regarding FasL, CTLs kill Fas^+ cells by exposing pre-formed FasL on the PM at the immunological synapse.[2] FasL induces crosslinking of the Fas death receptor on the target cell and apoptosis.[3] In CTLs, FasL is located at the limiting membrane of secretory lysosomes containing perforin/granzyme with MVB structure.[2] Upon T-cell receptor activation (TCR), MVBs undergo fusion with the PM, and relocalisation of FasL to the PM occurs.[2]

In addition to this transport of FasL, another mechanism for the delivery of FasL co-exists in CTLs.[4] This mechanism is because of the fact that FasL can be sorted from the limiting membrane of the MVBs to the ILVs by inward budding.[4,5] Upon cell activation, the fusion of preexisting MVBs with the PM results in the release of exosomes containing FasL.[5] In certain cells, such as Jurkat[6] or melanoma cells[7], this ILVs/MVBs pathway is the main mechanism involved in FasL traffic. Accordingly, a difference exists in FasL traffic between CTLs and non-CTL cells such as Jurkat. Although in both cell types, preformed and activation-induced synthesis of FasL coexist, in Jurkat cells the majority of FasL undergoes sorting to the ILVs in MVBs and is secreted into exosomes.[5] In addition, no PM relocation of FasL was observed in Jurkat,[5] J-HM1-2.2 (see ref. 8) or melanoma cells,[7] even in the presence of metalloproteinase inhibitors to avoid shedding of FasL from the cell surface.[9] This supports that, in contrast to FasL found in CTLs,[2] in Jurkat cells none or very little FasL is located in the limiting membrane of the MVBs.

Previous results have shown the role of diacylglycerol kinase α (DGKα), a diacylglycerol (DAG)-consuming enzyme,[10] on activation[11] and activation-induced cell death (AICD) of T lymphocytes.[8] AICD was defined as an autocrine suicide triggered by TCR stimulation, which controls lymphocyte homoeostasis,[12] that can be mimicked by muscarinic type 1 receptor (HM1R) stimulation with carbachol (CCh) in J-HM1-2.2 cells.[13] AICD requires *de novo* synthesis of FasL[12] and its secretion into exosomes.[6,8] Consequently, the kinetics for apoptosis initiation during AICD is slow (>4–5 h) when compared with CTL-mediated cytotoxicity, which occurs

[1]Instituto de Biologia y Genetica Molecular (IBGM), CSIC-Universidad de Valladolid, Facultad de Medicina, Valladolid, Spain; [2]Departamento de Bioquimica. Instituto de Investigaciones Biomedicas 'Alberto Sols', CSIC-UAM, Facultad de Medicina, Universidad Autonoma de Madrid, Madrid, Spain; [3]Cell Biology Unit, MRC Laboratory for Molecular Cell Biology, University College London, London, UK and [4]Centro Nacional de Biotecnologia, CSIC, Madrid, Spain
*Corresponding author: M Izquierdo, C-20, Instituto de Investigaciones Biomedicas 'Alberto Sols', CSIC-Universidad Autonoma de Madrid, c/Arturo Duperier, 4, 28029 Madrid, Spain. Tel: +34 91 4973117; Fax: +34 91 5854401; E-mail: mizquierdo@iib.uam.es
[5]These authors contributed equally to this work.
Keywords: T lymphocytes; diacylglycerol kinase α; multivesicular bodies; Fas ligand; exosomes
Abbreviations: Ab, antibody; AICD, activation-induced cell death; CCh, carbamyl choline (carbachol); CTL, cytotoxic T lymphocyte; DAG, diacylclycerol; DGK, diacylglycerol kinase; ESCRT, endosomal sorting complex required for transport; FACS, fluorescence-activated cell sorter; FasL, Fas ligand; HM1R, human muscarinic receptor type 1; HRP, horseradish peroxidase; mAb, monoclonal antibody; ILVs, intraluminal vesicles; LBPA, lysobisphosphatidic acid; MTOC, microtubule organising centre; MVBs, multivesicular bodies; PM, plasma membrane; SEE, Staphylococcal Enterotoxin E; TCR, T-cell receptor; TGN, trans-golgi network; WB, western blot
Received 02.8.10; revised 19.11.10; accepted 03.12.10; Edited by S Nagata; published online 21.1.11

in minutes. The inhibition of DGKα kinase activity increased the secretion of exosomes bearing FasL that was induced upon activation through TCR or the HM1R, a model for AICD.[8,13] Subsequently, the enhanced secretion of exosomes led to an increase in FasL-dependent AICD.[8] These results support that the effect of DGKα on apoptosis occurs by regulating the release of exosomes bearing *de novo*-synthesised FasL.[8] However, from these studies it was not clear whether stimulation of T lymphocytes affects the traffic of MVBs. In addition, the regulatory point(s) on secretory traffic of exosomes controlled by DGKα remained obscure.

Secretory vesicular traffic involves several checkpoints controlled by DAG at which cellular stimulation and DGKα might function. These include the fission of vesicles at the *trans*-golgi network, the generation and maturation of MVBs (i.e., number of MVBs per cell and inward vesiculation within MVB), the transport of the MVBs, and their docking and fusion to the PM.[14–17] To explore these possibilities, we have used pharmacological and genetic approaches.

Results

T-lymphocyte activation increases the formation of mature MVBs containing FasL. Stimulation of TCR or HM1R in J-HM1-2.2 cells induces apoptosis,[13] which occurs through the release of exosomes containing CD63 and *de novo*-synthesised FasL.[8] To explore the mechanisms involved in exosome secretion, we analysed the MVB markers CD63, Lamp-1 and the lipid lysobisphosphatidic acid (LBPA) in CCh-stimulated cells. Immunofluorescence analysis of CD63, FasL and LBPA showed that these markers were located in vesicles (Figure 1a). Comparable results were obtained in cells expressing CFP-CD63 (Figure 1b). The stimulation enhanced the number of $CD63^+$, $FasL^+$ or $LBPA^+$ vesicles (Figure 1a). To confirm this, a quantitative analysis was performed by flow cytometry and western blot (WB). As shown in Supplementary Figure S1, CCh increased the fluorescence of cells stained with anti-CD63, FasL or LBPA. The subcellular fractionation on Percoll gradients (Amersham Pharmacia, Piscataway, NJ, USA) has been used to analyse FasL into secretory lysosomes from CTLs[2] and MVBs from T lymphocytes.[8] The gradient from non-stimulated cells showed that $CD63^+$ and Lamp-1^+ fractions 12 and 13, which had the density of MVBs ($\rho = 1.05$–1.06 g/ml),[8,18] contained some preexisting FasL (Figure 2). Stimulation with CCh for 6 h, which upregulates the levels of FasL mRNA[13] and protein (Supplementary Figure S1), enhanced markedly the amount of FasL and CD63 in the fractions corresponding to MVBs[12,13] (Figure 2). Thus, cellular stimulation induces the recruitment of the upregulated FasL to subcellular compartments migrating at the same density that of MVBs.

Taken together, these results might represent an increase in the formation of mature MVBs upon cell activation. Not only to analyse this but also to stress whether the molecules found in the same fractions were present in the MVBs, we carried out analysis of LBPA in cells expressing CFP-CD63. LBPA constitutes a *bonafide* marker for ILVs of mature MVBs. As shown in Figure 1b, LBPA colocalised with CD63, and stimulation with CCh increased the number of $LBPA^+CD63^+$ vesicles (Supplementary Figure S2). Thus, the biochemical and immunofluorescence results, together with the published results showing colocalisation of FasL with CD63 and lamp-1,[5] supported that, upon CCh stimulation, there was an increase in the number of mature MVBs containing CD63, LBPA and FasL.

To confirm that these vesicles exhibited MVBs ultrastructure, we analysed the cells by electron microscopy. As shown in Supplementary Figure S3, stimulation with CCh increased the number of vesicles containing an electron-dense content, with the features of MVBs observed in CTLs[19] and T lymphocytes.[5] Taken together, the data support that stimulation of cells increased the number of mature MVBs that contain FasL. We examined next the contribution of DGKα to the biogenesis of MVBs and exosomes.

Inhibition of DGKα kinase activity increases the number of mature MVBs. Fractionation on Percoll gradients has revealed the presence of DGKα in $CD63^+$ late endosome fractions from non-stimulated cells.[20] Similar analysis following CCh treament revealed that the increase in DGKα levels in these fractions mirrored those of CD63 and FasL, suggesting that stimulation enhances the formation of DGKα-enriched MVBs (Figure 2). We have shown that inhibition of DGKα kinase activity increased exosome release.[8] As CCh enhances association of DGKα with subcellular fractions containing MVBs, we analysed the influence of DGKα kinase activity on the formation of MVBs upon stimulation. Treatment of the cells with the inhibitor of type I DGKs R59949 (see ref. 21) enhanced the number of exosomes secreted in non-stimulating conditions as determined by FACS; this effect was stronger in response to CCh (from 6481 up to 9410 events) (Figure 3a). DGKα inhibition resulted in higher levels of CD63 and its redistribution in fractions containing MVBs (Figure 3b), and enhanced the ability of CCh to increase the number of vesicles decorated with CD63 and the number of $LBPA^+$ vesicles (Supplementary Figure S4). The vesicles induced by CCh in the presence of R59949 displayed the features of MVBs (Supplementary Figure S3), and contained both CFP-CD63 and LBPA (not shown). Together, these data indicate that the inhibition of DGKα kinase activity enhances the formation of $CD63^+$, $LBPA^+$ mature MVBs, which correlates with the enhanced release of exosomes.

Inactive DGKα colocalises with MVBs. Previous experiments demonstrate that DGKα is found in subcellular fractions containing MVBs, and suggest a negative function of DGKα kinase activity in the formation of mature MVBs. If this is the case, then DGKα might be found associated with the limiting membrane of MVBs, sorted to the ILVs and then secreted in exosomes. We have demonstrated that DGKα localisation is negatively regulated by its own kinase activity, as R59949 enhances association of DGKα to membranes.[11] Therefore, we used confocal microscopy to investigate the effect of the inhibition of DGKα kinase activity on DGKα localisation. CCh in the presence of R59949 induced, in addition to the described translocation of GFP-DGKα to the

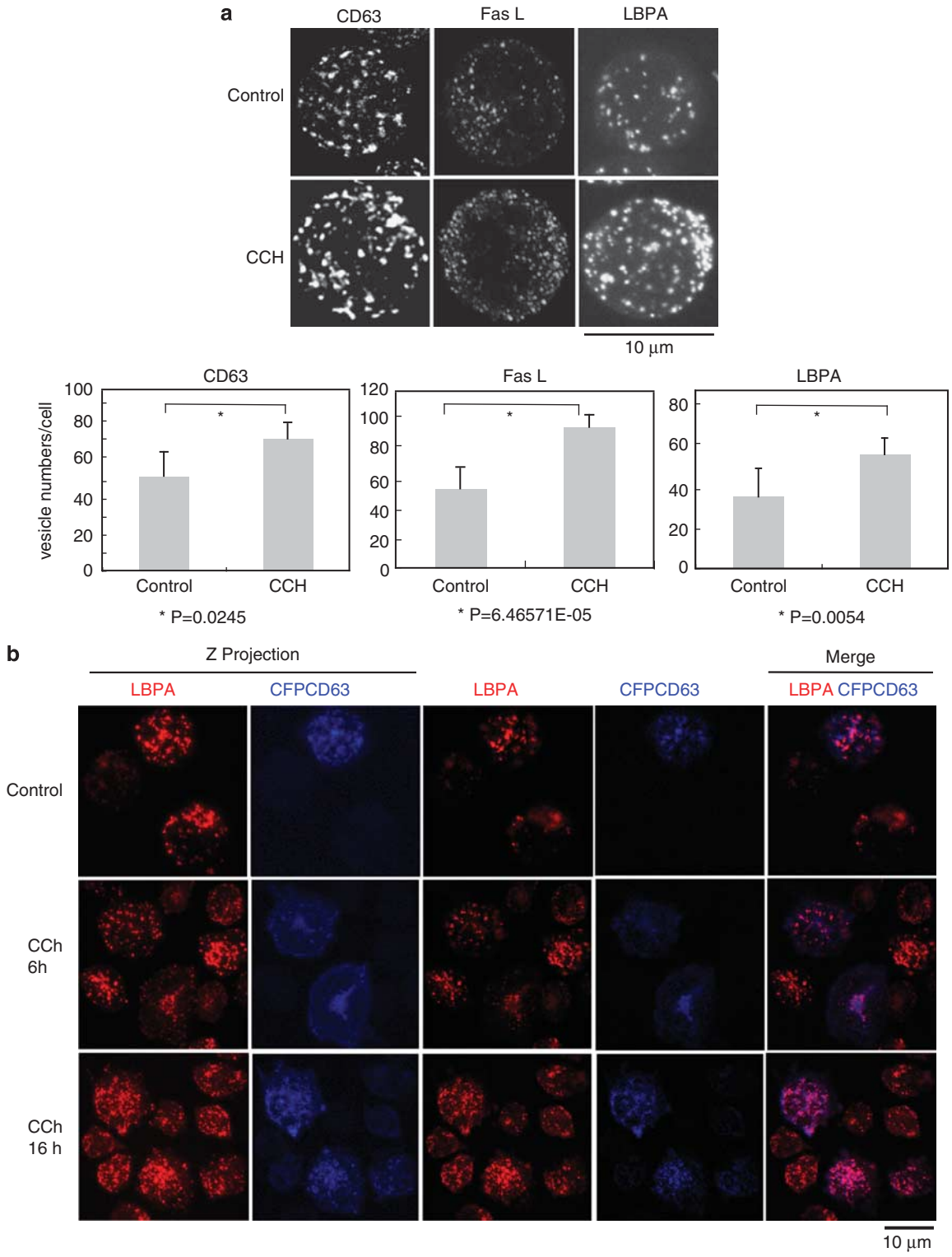

Figure 1 Cellular stimulation induces the formation of mature MVBs. (**a**) Upper panel, J-HM1-2.2 cells were stimulated with CCh for 6 h and then were imaged by confocal microscopy using antibodies specific for CD63, FasL and LBPA. Lamp-1 is mostly present on the limiting membrane of MVBs, whereas CD63, and particularly LBPA, are abundant in the ILVs,[27] and therefore label mature MVBs. LBPA is a phospholipid that participates in the maturation of MVBs[33] and constitutes a *bonafide* marker for ILVs of mature MVBs.[33] The *z*-axis projections for each antigen corresponding to representative cells from three independent experiments are represented. Lower panel shows quantitative analysis of vesicles. Vesicle numbers were recorded from at least 20 cells per group, chosen randomly as indicated in Materials and Methods. Results represent average number of vesicles/cell ± S.D. of three independent experiments. (**b**) J-HM1-2.2 cells, transfected with CFP-CD63, were stimulated with CCh (for 6 and 16 h), and mature MVBs were visualised with anti-LBPA antibody (red) as indicated in Materials and Methods. Cells were imaged by confocal microscopy and representative ($n = 3$ independent experiments), single optical sections (0.4 μm thick) and merged images (coincident labelling appearing pink) are shown in the right side. In the left side, *z*-axis projection images of LBPA and CFP-CD63 are shown

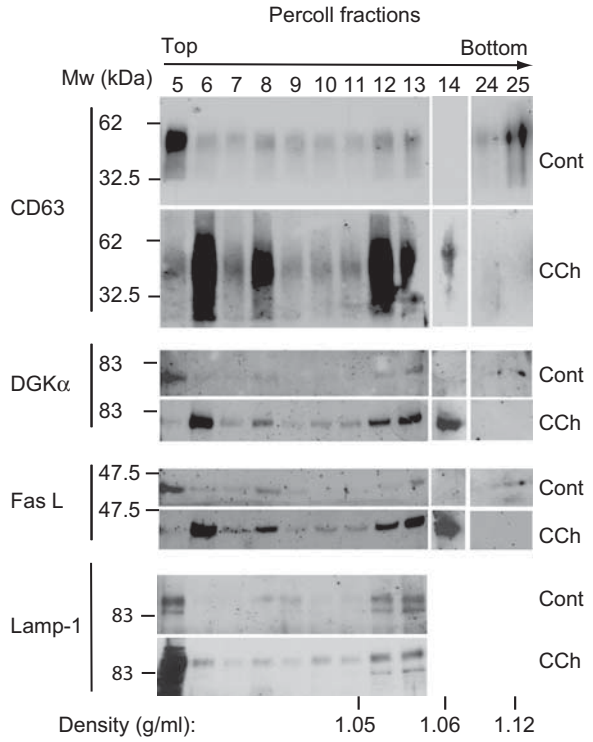

Figure 2 Cellular stimulation induces the relocalisation of FasL and DGKα to subcellular fractions containing MVBs. Cellular fractionation by density gradient of the homogenates from equal numbers of J-HM1-2.2 cells, stimulated or not stimulated with CCh (6 h), was performed as indicated in Materials and Methods, and the Percoll fractions were analysed for CD63, DGKα and FasL by WB. The blot was reprobed with anti Lamp-1 antibody as a loading control. Data are representative of the results obtained in three different experiments

PM,[11] the accumulation of GFP-DGKα in vesicles, most of them being CD63$^+$, distributed throughout the cytoplasm (Figures 4a and b, arrows). As R59949 enhanced the release of exosomes,[8] and induced the formation of mature (CD63$^+$ LBPA$^+$) MVBs (Supplementary Figure S4), we analysed by WB, the exosomes secreted from cells stimulated with CCh, in the presence or the absence of R59949, for the presence of DGKα. As shown in Figure 4c, the amount of DGKα secreted in the exosomes mirrored the increase corresponding to other proteins (i.e., CD63) or inducible FasL (compare CCh 500 with CCh 500 plus R59949).

Traffic of MVBs. To analyse the contribution to exosome secretion of the transport and fusion of MVBs to the PM, and to assess the effect of DGKα on these events, we analysed the traffic of MVBs. To this end, we used expression vectors for the MVB/exosome marker CD63 fused to GFP, DsRed2 or CFP. As shown in Figure 5a, CCh enhanced the amount of GFP-CD63$^+$ and DsRed2-CD63$^+$ exosomes secreted by transfected cells, as seen with endogenous CD63 (Figure 4c). Once the reporters were validated, we analysed the formation and traffic of MVBs containing the reporters in living cells. The expression of GFP-CD63 in non-stimulated cells revealed vesicles distributed all over the cytoplasm, and the PM was weakly stained with GFP-CD63 (Figure 5b, upper panels). Time-lapse microscopy showed a myriad of CFP-CD63$^+$ vesicles undergoing a rapid movement inside the cytoplasm (Supplementary Videos 1 and 2). Particularly upon CCh stimulation, these vesicles exhibited bidirectional motion emerging from the pericentriolar area. Stimulation with CCh for 24 h, increased the intensity of the labelling, the number of these granules and their dispersion within the cell (Figure 5b, Supplementary Videos 1 and 2). In addition, stimulation for 6 h enhanced the staining of GFP-CD63 at the PM (Figure 5b). Some of the scattered granules appeared as ring-shaped vesicles (Supplementary Video 4, zoom in Figure 5b), brightly labelled with the chimera at the peripheral membrane. Time-lapse microscopy showed that, upon stimulation some vesicles approached, seemed to dock to the PM and disappeared (Supplementary Videos 3 and 4); these observations are compatible with the fusion of the MVBs to PM.

Next, we studied the role of DGKα pathway on the formation and fate of MVBs. R59949 enhanced the fluorescence of the intracellular vesicles and the accumulation of GFP-CD63 in the PM upon CCh stimulation for 6 h (Figure 5b). The CCh and R59949-induced increase in GFP-CD63 at the PM was because of the fusion of the limiting membrane of GFP-CD63$^+$ MVBs (Supplementary Videos 3 and 4). This increase in GFP-CD63 at the PM combined with increased number of CD63$^+$ and LBPA$^+$ vesicles, which were induced by CCh and R59949 (Figures 1, 3, and Supplementary Figures S2 and S4), and the enhanced secretion of GFP-CD63$^+$ exosomes (Figure 5a), support that the inhibition of the kinase activity of DGKα increases the formation of mature MVBs, containing intraluminal CD63$^+$/LBPA$^+$ vesicles. In addition, as shown in overexposed blots (Figure 5a), R59949 enhanced the constitutive secretion of exosomes containing GFP-CD63 as previously reported with endogenous CD63.[8]

Overexpression of DGKα inhibits the formation of mature MVBs. If the effect of R59949 is exerted through the inhibition of DGKα kinase activity, it would be expected that overexpression of the enzyme would decrease the number of mature MVBs, leading to a reduction in exosome secretion.[8,20] To study the number of mature MVBs, we analysed the distribution of CD63 and LBPA in cells co-transfected with CFP-CD63 and GFP-DGKα, GFP-VPS4wt and GFP-VPS4EQ. The expression of a VPS4 ATPase-defective mutant, VPS4EQ, constitutes a control for aberrant MVBs maturation.[22,23] As shown in Figure 6, GFP-VPS4wt was cytosolic, whereas VPS4EQ accumulated in a few, bright-fluorescent foci that co-localised with CFP-CD63 and LBPA (Figure 6 and Supplementary Figure S5), with the appearance of enlarged, ring-shaped vesicles. There was a reduction in the number of LBPA$^+$ vesicles in GFP-VPS4EQ$^+$ cells when compared with non-transfected cells or GFP-VPS4wt$^+$ cells (Figure 6). CCh stimulation of non-transfected cells or GFP-VPS4wt$^+$ cells increased the number and the labelling of the LBPA$^+$ vesicles. In contrast, upon stimulation of GFP-VPS4EQ$^+$ cells, the number of LBPA$^+$ vesicles remained low and few, enlarged LBPA$^+$ vesicles were observed (Figures 6a and c). The number of LBPA$^+$ vesicles was reduced in non-stimulated cells expressing GFP-DGKα (Figure 6a); this effect was striking upon CCh stimulation (Figures 6a and c).

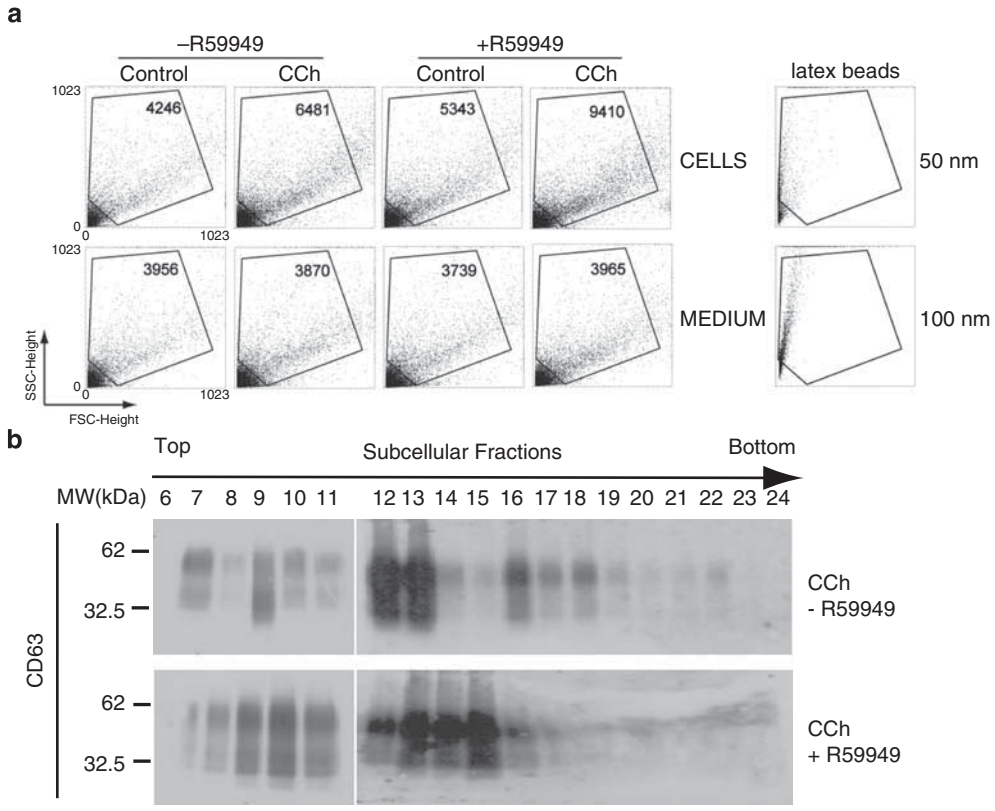

Figure 3 Inhibition of DGKα kinase activity increases the number of MVBs and the secretion of exosomes. (**a**) The secretion of exosomes was induced by treatment of J-HM1-2.2 cells with CCh during 10 h, preincubated or not with R59949 (10 μM). In the upper row, the dot plots correspond to the events recorded – the number of events is included inside each plot – in the cell culture supernatants from cells treated as indicated, whereas the lower row plots register the events from complete medium treated with different reagents but in the absence of cells. The lower row dot plots registered a constant number of events; thus events above this background should be considered as specific, cell-produced vesicles. In the right-hand side, dot plots corresponding to 50 and 100 nm latex beads, analysed in parallel, are included as a reference. (**b**) WB with anti-CD63 of Percoll density gradient fractions from cells stimulated with CCh for 6 h, pretreated or not with R59949. Data are representative of the results obtained in three different experiments. The shift in the distribution of CD63 on the density gradient is compatible with changes in the lipid composition and the maturation of MVBs[27]

With regard to the effect of DGKα on the traffic of CD63-containing vesicles, the analysis of CD63 relocation at the PM, induced by CCh stimulation, showed no differences between GFP-DGKα$^+$ and GFP-DGKα$^-$ cells (Figure 6b, top panels) at several time points; the same result was observed in VPS4EQ$^+$ cells (Figure 6b, lower panels). Thus, the expression of DGKα or VPS4EQ seemed not to affect the transport, docking and fusion of the CD63$^+$ vesicles to the PM in a non-polarised model of secretion.

The recognition of target cells by CTLs induces polarisation of MVBs towards the immune synapse, and the polarised transport, docking and fusion of MVBs with the PM at the synapse.[2] Therefore, the accumulation of CD63 at the PM in a synapse model provided information to extend the findings regarding the role of DGKα on secretion to a polarised situation. To perform these experiments, we used Raji cells presenting Staphylococcal Enterotoxin E (SEE) to Jurkat cells[24] expressing GFP-CD63. As seen in Supplementary Figure S6, recorded 5 h after synapse formation, there was an accumulation of GFP-CD63$^+$ vesicles close to the synapse; the movement of vesicles in and out from this area was recorded (Supplementary Videos 5 and 6, Supplementary Figure S6). In addition, an accumulation of GFP-CD63 in the cell surface was observed. We verified that overexpression of DGKα was inhibited, and the inhibition of DGKα increased the secretion of exosomes in the synapse (Figure 7), as seen in the non-polarised model (compare Figure 7 with Figures 4c and 5a). Subsequently, we tested that R59949 specifically reverted the inhibition on exosome secretion exerted by DGKα but not by DGKζ, as the inhibitor partially rescued the inhibitory effect of DGKα on exosome secretion, but not the effect corresponding to DGKζ (Figure 7).

The absence of DGKα inhibits the polarised traffic of MVBs. As it is possible that the absence of DGKα may exert a different effect on secretion when compared with the inhibition of the kinase activity of DGKα, we analysed polarised traffic and secretion in cells lacking DGKα. As seen in Figure 8a, pSuper-siRNA humanDGKα plasmid reduced the amount of DGKα protein when compared with non-relevant plasmids (Figure 8a). This seemingly low reduction was more pronounced when DGKα was analysed in selected GFP$^+$ cells (Figure 9b). The interference on DGKα inhibited the polarised secretion of GFP-CD63$^+$ exosomes induced by SEE (Figures 8b and c). We aimed to reveal traffic events underlying the effect of DGKα

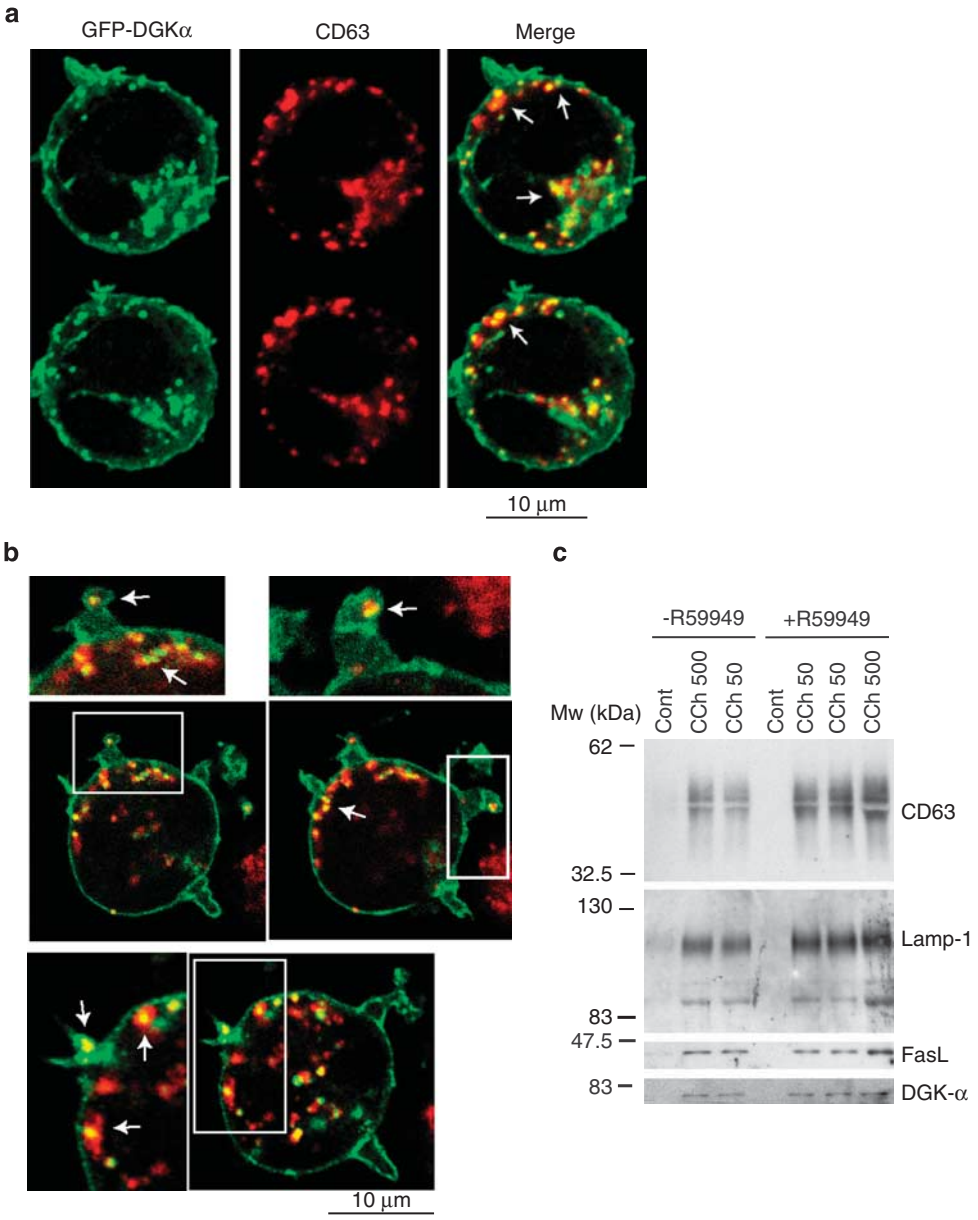

Figure 4 DGKα is associated to CD63$^+$ vesicles and exosomes. (**a**) Cells expressing GFP-DGKα were stimulated with CCh for 6 h in the presence of R59949, stained with anti-CD63 (red), and cells were imaged by confocal microscopy; several representative, optical sections (0.4 μm thick) are shown. The right-hand panels show the merged images, with coincident labelling appearing yellow. (**b**) Digital zoom (× 1.67) of some images from one experiment similar to that described in panel a are shown. (**c**) Cells were stimulated or not stimulated with CCh (50 and 500 μM) for 12 h in the presence or absence of R59949 (10 μM), and the secreted exosomes were analysed by WB for the presence of several exosome markers and endogenous DGKα. Results are representative of the data obtained in three different experiments

interference on secretion. Thus, we analysed the relocation of endogenous CD63 to the synapse, which is consequence of the degranulation of MVBs.[2] As seen in Figure 9a, upon stimulation with SEE for 1 or 5 h, the interfered GFP$^+$ cells had low levels of cell surface CD63 when compared with GFP$^-$ cells, as assessed by flow cytometry (Figure 9a, lower panel). The absence of DGKα did not affect the formation of mature MVBs, as the number of MVBs per cell remained unchanged (Figure 9b). As degranulation of MVBs was inhibited in the absence of DGKα, but both the formation of synapses and number of MVBs remained unaffected, we analysed the ability of DGKα$^-$ cells to polarise MVBs. To this end, we labelled DGKα, together with intracellular CD63 or LBPA. As seen in Figure 9b, GFP$^+$ cells lacking DGKα and stimulated for 1 or 5 h were unable to polarise CD63$^+$ or LBPA$^+$ granules (not shown) towards the synapse, when compared with either GFP$^-$DGKα$^+$ or GFP$^+$DGKα$^+$ cells. Therefore, most probably, an inhibition of polarisation of mature MVBs towards the synapse underlied the effect of DGKα interference on secretion of exosomes.

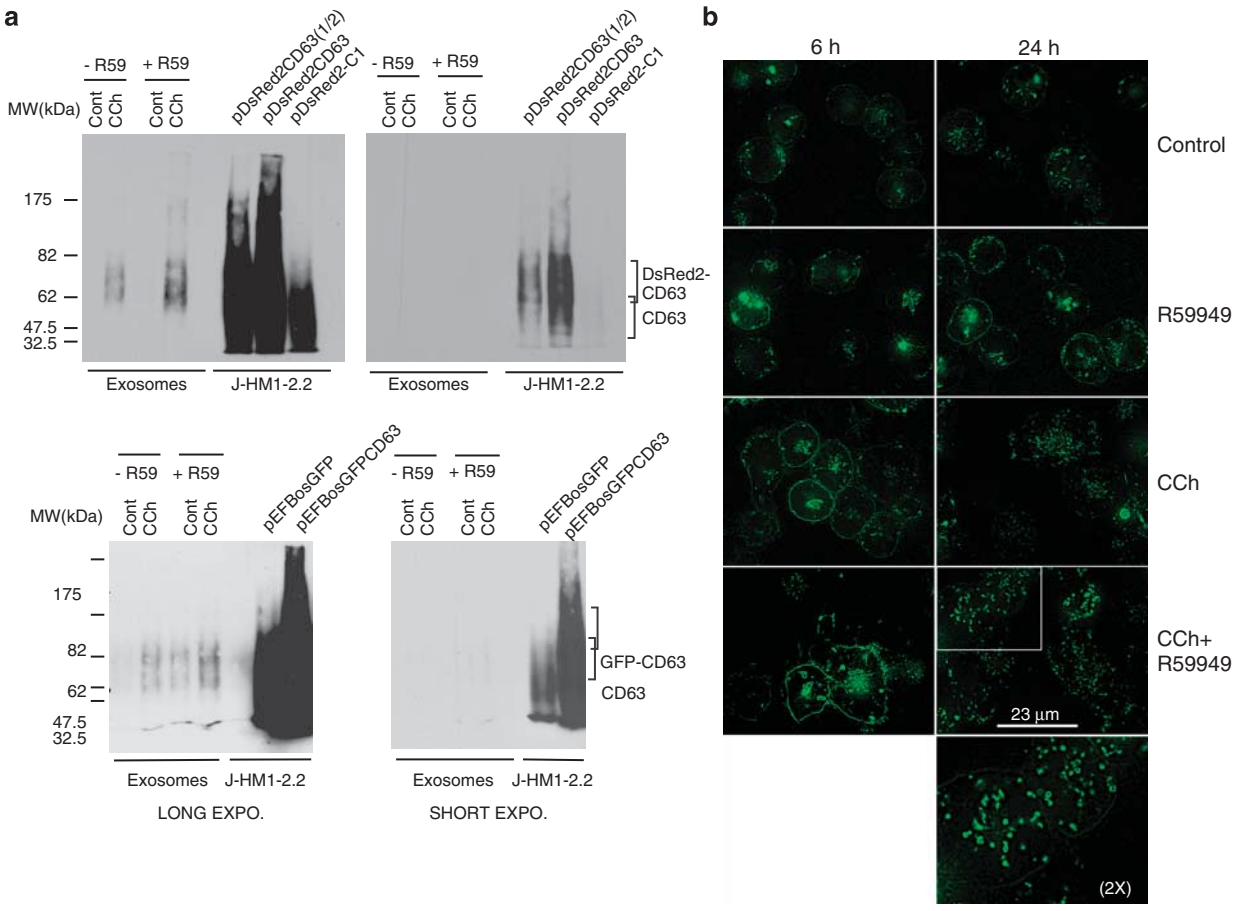

Figure 5 Expression of the reporters for MVBs/exosomes in living cells. (**a**) J-HM1-2.2 cells expressing DsRed2-CD63 (upper panels) or GFP-CD63 (lower panels) were stimulated with CCh for 10 h in the presence or the absence of R59949 inhibitor (R59, 10 μM), and the isolated exosomes were analysed by WB with anti-CD63 to detect the chimerical CD63 molecules. Different exposures of the same blot are shown to visualise both the chimeras and the endogenous CD63. In the right-side lanes of each blot, lysates from cells expressing or not expressing the CD63 chimeras were run as a reference. (**b**) Cells expressing GFP-CD63 were stimulated or not expressing with CCh for 6 and 24 h in the presence or the absence of R59949 to visualise the formation and fate of MVBs in living cells. The CCh- and R59949-induced increase in GFP-CD63 at the plasma membrane was probably because of the fusion of the limiting membrane of GFP-CD63$^+$ MVBs (see also Supplementary Videos 3 and 4). The epifluorescence images were improved by image deconvolution as indicated in Materials and Methods, and are representative of the results obtained of more than 50 cells recorded per treatment in four independent experiments. The inset shows a $\times 2$ digital zoom of the indicated area

Discussion

Our data support that T-lymphocyte activation increases the number of mature MVBs that contain FasL on their ILVs. Besides this effect of cell activation on formation of mature MVBs, an increase in mobilisation, docking and fusion of these MVBs to the PM might underlie the stimulated release of FasL-bearing exosomes. The inhibition of DGKα kinase activity, previously shown to enhance exosome secretion,[8] also increases the formation of mature MVBs induced upon activation. However, we could not rule out a nonspecific effect of the inhibitor. Thus, we tested that the inhibitor acted on DGKα, but not on DGKζ, as the inhibitor did not rescue DGKζ-induced inhibition of exosome secretion (Figure 7). To examine a possible negative function of DGKα kinase activity in the transport, docking and fusion of MVBs with the PM, we overexpressed DGKα and analysed these events. We observed that DGKα negatively regulated the formation of mature MVBs, but did not appear to affect their subsequent traffic. In contrast, the association of DGKα with MVBs, the effect of DGKα on the formation of mature MVBs, the association of DGKα with exosomes and its role on exosome secretion, are compatible with the idea that DGKα kinase activity is an important negative regulator of the formation of MVBs. The fact that inhibition of DGKα kinase enhances the number of mature MVBs and partially rescues the inhibition of exosome secretion, conferred by DGKα overexpression, supports the notion of DGKα kinase activity function as an important negative regulator of polarised and non-polarised exosome release. In addition to the positive effect of the inhibitor on the inducible secretion, we observed also a positive effect on the constitutive secretion of exosomes (Figures 3a and 5a).[8] It is known that there is constitutive DAG production at intracellular membranes.[25] This DAG pool is necessary for constitutive vesicular traffic,[15] and R59949 has been shown to enhance basal DAG levels on

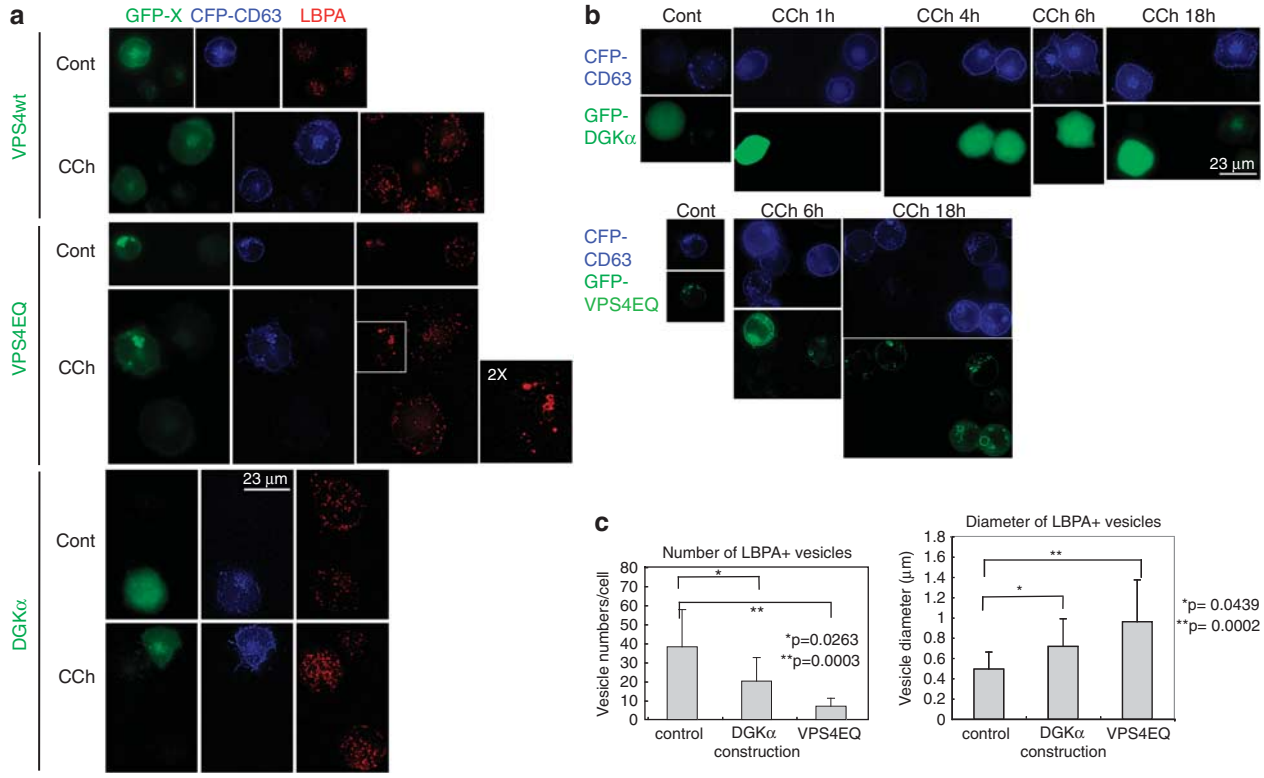

Figure 6 Expression of GFP-DGKα affects the formation of mature MVBs and the distribution of LBPA$^+$ vesicles, but does not inhibit the accumulation of CD63 at the plasma membrane. Jurkat cells expressing GFP-VPSwt, GFP-VPS4EQ mutant or GFP-DGKα, together with CFP-CD63, were stimulated with CCh to induce the formation and traffic of MVBs, and LBPA was stained as indicated in Materials and Methods. The endosomal sorting complex required for transport (ESCRT) machinery is involved in the formation of the intraluminal vesicles of MVBs, and the AAA-ATPase vacuolar protein-sorting VPS4 regulates the recycling of the ESCRT complexes.[34] The expression of a VPS4 ATPase-defective mutant, VPS4EQ, inhibits the inward budding at the limiting membrane of MVBs and the subsequent formation of ILVs.[22,35] These effects result in the formation of immature, large endosomes,[22,23] and thus the expression of VPS4EQ mutant constitutes an appropriate control for aberrant MVBs maturation. (**a**) Epifluorescence microscopy images (GFP-X, CFP-CD63 and LBPA, respectively) of control and CCh-stimulated (8 h) cells. In GFP-VPS4EQ-expressing cells, the dispersion of LBPA$^+$ granules that was induced by CCh in GFP-VPS4EQ cells or in cells expressing GFP-VPS4wt was inhibited, and the large LBPA$^+$ structures accumulated in the perinuclear area. (**b**) Cells expressing GFP-DGKα (upper rows) or GFP-VPS4EQ (lower rows), together with CFP-CD63 were stimulated with CCh for the indicated times to visualise the accumulation of CFP-CD63 at the plasma membrane by fluorescence microscopy. CD63 cell surface labelling is a consequence of the transport, docking and fusion of MVBs with the plasma membrane (see also Figure 5b, Supplementary Videos 3 and 4). (**c**) The average number per cell and the mean diameter (± S.D.) of LBPA$^+$ vesicles were measured in cells from three independent experiments similar to that described in panel a (in a total of 11 control, untransfected cells; 8 GFP-DGKα$^+$ cells; and 19 GFP-VPS4EQ$^+$ cells) after 6 h of CCh stimulation. In a significant fraction (40–50%, $n = 20$ cells) of GFP-DGKα-expressing cells, the number of LBPA$^+$ vesicles was lower to that found in GFP-DGKα$^-$ cells stimulated with CCh (Supplementary Figure S5, panel A, third row). In approximately 20% of GFP-DGKα$^+$ cells, the LBPA$^+$ structures were condensed in some areas but not dispersed throughout the cytosol (Supplementary Figure S5, panel A, lower row), as observed in GFP-VPS4EQ$^+$ cells (Supplementary Figure S5, panel A, second row). See also Supplementary Figure S5, panel C

endomembranes,[25] probably by inhibition of DGKs. Thus, it is conceivable that the inhibitor –by affecting intracellular DAG pools– might positively control the constitutive traffic of MVBs, and subsequently, the basal secretion of exosomes.

We investigated the role of DGKα in the polarised secretion of exosomes. By using an interference approach on a synapse model, we uncovered a positive role of DGKα on exosome secretion. In DGKα-interfered cells, polarisation of MVBs and subsequent exosome release were reduced (Figure 9). This, together with the fact that the kinase inhibitor increases polarised secretion of exosomes (Figure 7) implies that some non-kinase function of DGKα is required for polarised secretion. The fact that R59949 partially rescues the negative effect of DGKα overexpression on exosome secretion (Figure 7), along with the inhibitory effect that DGKα downmodulation produces on MVBs polarisation and degranulation (Figures 8 and 9), suggest that different functional domains of DGKα negatively and positively control the secretory traffic of exosomes at, at least, two distinct regulatory points. Whereas the kinase domain appears to be negatively involved in formation of mature MVBs, other(s) domain(s) would be positively involved in MVBs polarisation. Although both the nature of these domains and their effectors remain unknown, our results point out to a complex, fine-tuned control of the secretory traffic of exosomes exerted by DGKα.

The lipid composition of vesicles constitutes a factor in the maturation of MVBs that is susceptible to regulation by DGKα. The contribution of LBPA is of interest, as LBPA provides negative curvature to the MVB-limiting membrane during the inward invagination to form the ILVs.[26] In the latter study, it has been shown that ALIX, a protein that interacts with ESCRT complexes, binds to LBPA-containing liposomes. When ALIX levels were downregulated, the formation of LBPA-containing endosomes decreased.[26] Thus, ALIX

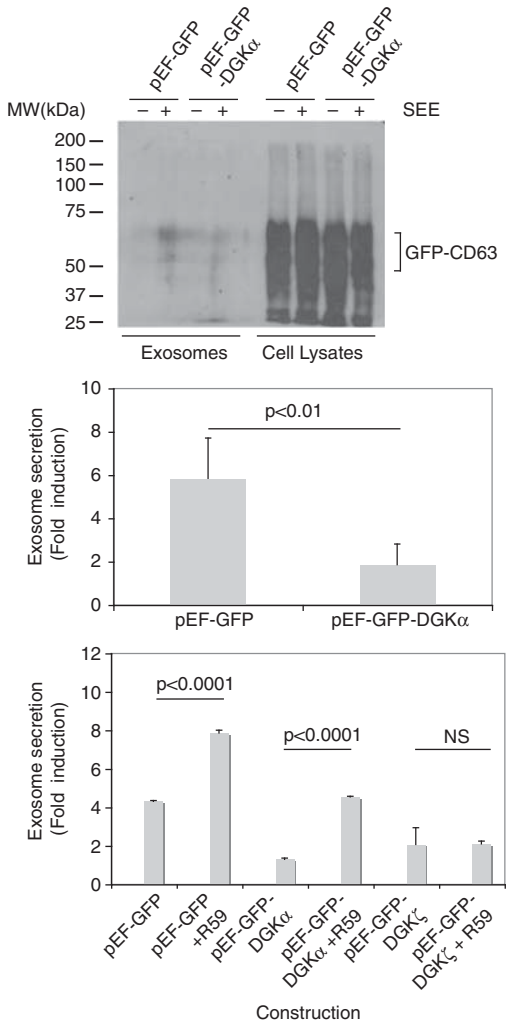

Figure 7 Modulation of DGKα pathway controls the polarised secretion of exosomes. Jurkat cells co-expressing GFP-DGKα or GFP, together with GFP-CD63, were mixed with Raji cells, pulsed or not with SEE, to induce the formation of synapse and the secretion of exosomes. Upper panel: the amount of exosomes produced by cells expressing similar amounts of GFP-CD63 (cell lysates, right side) at the end of the culture period was measured by WB with an antibody against CD63. Middle panel: quantification of the secretion of exosomes in cells expressing GFP-DGKα in comparison with cells expressing GFP. Results summarise the data obtained from WB in four independent experiments and are represented as average (± S.D.) fold induction of exosome secretion. Lower panel: the effect on exosome secretion of the pretreatment with R59949 (10 μM) of cells expressing GFP (control), GFP-DGKα or GFP-DGKζ was measured as indicated in the middle panel ($n = 3$ independent experiments)

regulates the maturation of MVBs. LBPA is locally produced in MVBs,[26] but the steps involved in LBPA synthesis remain unclear. Therefore, it will be interesting to analyse the consequences of the regulation of DAG levels by DGKα on both the synthesis of LBPA and the recruitment of ALIX/ESCRT to the MVBs. One possibility that might explain the inhibition of exosome secretion by DGKα, and the fact that DGKα overexpression inhibits the formation of LBPA$^+$ vesicles is that the enzyme would affect the maturation (number of ILVs) of MVBs. If this is the case, then DGKα could be found associated with the MVBs and secreted in exosomes, as we have shown. Thus, quite probably, DGKα controls the inward budding in MVBs. The changes induced by R59949 in the distribution of CD63 on gradients (Figure 3b) support this hypothesis, as the maturation of late endosomes/MVBs is associated with an increase in their content in LBPA, which confers a shift in the density of MVBs.[27]

Apart from this potential role of DGKα on the lipid composition of MVBs, it is conceivable that DGKα activity might affect the gradient of DAG at the synapse; this gradient is crucial for MTOC polarisation in CTLs.[17] DGKα relocates to the PM upon cell activation and regulates the intensity of signalling of DAG-controlled pathways in T lymphocytes,[11] thus it is conceivable that DGKα may contribute to maintain a DAG gradient at the synapse. Loss of this gradient, as a result of DGKα downregulation, could be responsible for the defect in MVBs polarisation and degranulation. However, our data showing that R59949 increases polarised secretion of exosomes rules out that the inhibition of polarised secretion in DGKα-interfered cells might be because of the absence of DGKα kinase activity that would otherwise control a DAG gradient at the PM. Our results describing an increment in exosome secretion by treatment with R59949 are in apparent contradiction with the studies by Quann *et al.*,[17] showing that DGK kinase activity is required to maintain a stable DAG gradient. Treatment of CTLs with R59949 induced a defect in the persistence of both MTOC polarisation and the secretion of cytolytic factors towards the synapse and CTL-mediated killing.[17] The divergence may be because of the fact that mouse CTLs, instead of human cell lines, were used in that study;[17] and no evaluation of the secretion of exosomes and their contribution to apoptosis was performed. In addition, in DGKα-overexpressing cells, the secretion of exosomes is reduced, and there are few CD63$^+$LBPA$^+$ vesicles per cell. However, the MVBs are transported, docked and fused normally with the PM in cells overexpressing DGKα. Thus, the inhibition of the formation of mature MVBs appears to be the limiting step in secretory traffic of exosomes, at least in cells overexpressing DGKα. As GFP-DGKα translocates to the PM, it is conceivable that the gradient of DAG at the synapse, which may control MVBs polarization,[17] is maintained in these cells. In contrast, in DGKα-interfered cells, the defective polarisation of MVBs would constitute a different limiting step for exosome secretion. Experiments involving the use of 'caged' dioctanoylglycerol,[17] photoactivable at different locations (synapse, MVBs), and the expression of DAG sensors, such as C1 domains of PKCθ fused to GFP,[25,28] might help to evaluate spatio–temporal changes of DAG levels, both in DGKα-overexpressing and in DGKα-interfered cells, and to study the consequences of these changes on traffic of MVBs and exosome secretion.

Taken together, our data support the idea that the combination of positive signals triggered by receptor stimulation and a fine-tuning effect of a negative regulator, that is, the kinase activity of DGKα control the secretory vesicle pathway that is responsible for the secretion of exosomes. The negative effect of DGKα kinase activity on traffic was exerted at the stage of formation of mature MVBs. In addition, a non-kinase function of DGKα is necessary for polarisation of MVBs and exosome secretion. These inferences might conciliate the DGKα interference data, with the fact that R59949 kinase

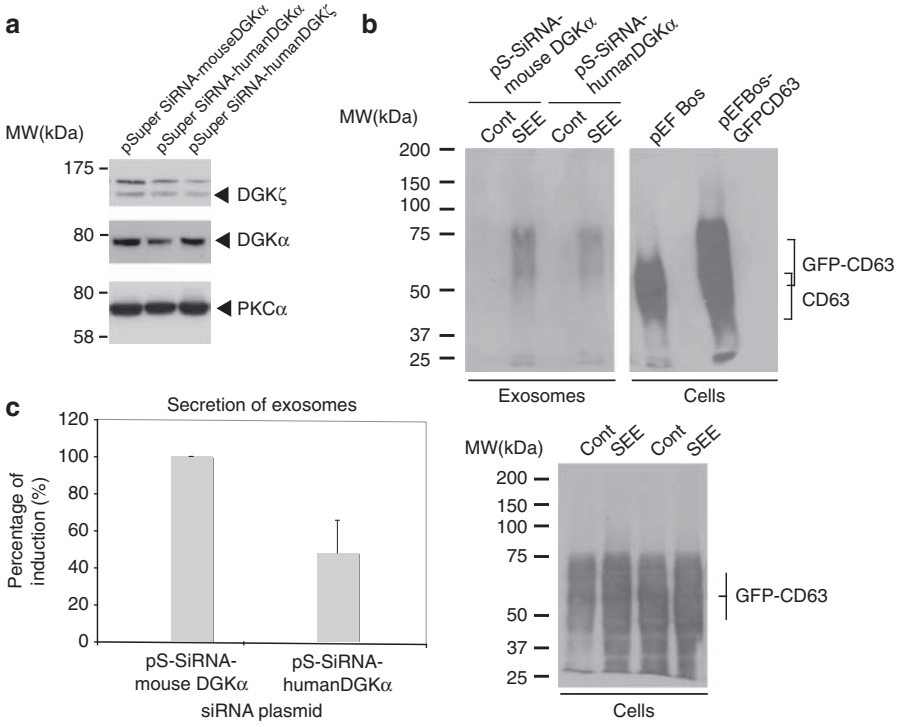

Figure 8 Interference of DGKα inhibits polarised exosome secretion. Jurkat cells were co-transfected with interference plasmids for human DGKα, human DGKζ, or an irrelevant, mouse DGKα, together with reporter GFP-CD63, and were stimulated with Raji cells, pulsed or not (control) with SEE, to induce secretion of exosomes. Transfection efficiency of Jurkat cells in these experiments was around 50%, as assessed by flow cytometry. (**a**) WB of Jurkat cells transfected with the interference plasmids before stimulation with Raji cells, showing the specificity of the interference with specific antibodies against DGKα and DGKζ. (**b**) WB of the exosomes (upper panel) isolated from the cell culture supernatants of the interfered cells after synapse formation (12 h). In the right side, extracts of cells transfected with an empty vector and a GFP-CD63 vector were analysed as reference. The WB of the cells (lower panel) recovered after the culture period was performed in parallel to normalise by viable cell number at the end of the culture period and by transfection efficiency of the GFP-CD63 reporter. (**c**) Summary of the results from four independent experiments similar to the one shown in panel **b**; results are represented as average (± S.D.) percent of SEE induction of exosome secretion

inhibitor enhances polarised secretion and rescues the negative effect of DGKα overexpression on exosome secretion. Thus, DGKα appears to coordinate both positive and negative signals that are exerted at two different stages of the traffic of MVBs; the balance of these signals seems to be crucial for exosome secretion.

Materials and Methods

Cell cultures. J-HM1-2.2 cells expressing HM1R have been described;[29] these cells stimulated with agonist CCh have been widely used as an appropriate model to induce full activation signals[11] and AICD.[13] Raji B cell line was from ATCC (Teddington, UK).

Antibodies and reagents. The anti-DGKα antibody (Ab) for WB and immunofluorescence was from Abnova (Taipei City, Taiwan). Anti-FasL (CD95L) NOK-1 mAb, anti-Lamp-1 (clone 25), anti-CD3 (UCHT1) and anti-FasL G247-4 for immunofluorescence were obtained from BD Biosciences (San Jose, CA, USA) and Santa Cruz Biotechnology (Santa Cruz, CA, USA). Rabbit polyclonal anti-FasL (CD95L) Q-20 for WB was from Santa Cruz Biotechnology. Anti-CD63 (clone NKJ-C-3) was from Oncogene (Darmstadt, Germany). Anti-Golgi 58K protein (clone 58K-9) was from Sigma (Lyon, France). Anti-LBPA Ab 6C4 was a kind gift from Dr. J Gruenberg. All horseradish peroxidase-coupled secondary antibodies were from Dako (Glostrup, Denmark). Carbachol was from Sigma. The DGK inhibitor II (R59949) was purchased from Calbiochem (Darmstadt, Germany). This inhibitor is specific for the type-I DGK isotypes (as DGKα) but does not inhibit DGKζ (see ref. 10,21) (the other DGK isotype expressed in T lymphocytes[30]). Alexa Fluor-coupled secondary antibodies were from Invitrogen (Carlsbad, CA, USA). Staphylococcal Enterotoxin E was from Toxin Technology, Inc. (Sarasota, FL, USA). Cell tracker blue (CMAC) was from Invitrogen.

Expression vectors, siRNA interference vectors and transfection assays. The plasmids pEFbos-GFP, pEFGFP-DGKα, pEFGFP-DGKζ have been described.[8,11,30] pEFGFP-C1bosCD63 and pECFP-C1CD63 were a generous gift from Dr. G Griffiths. pDsRed2-CD63 was prepared by subcloning cDNA corresponding to human CD63 from pEFGFP-C1bosCD63 into pDsRed2-C1 vector (BD Biosciences). Expression vectors for GFP-VPS4wt and GFP-VPS4EQ mutant were a gift from Dr. P Whitley.[31] siRNAs expression was achieved by using pSUPER RNAi System (pSR-GFP bicistronic or pSuper plasmids) (Oligoengine, Seattle, WA, USA). One sequence of human DGKα isoform was selected to generate 64 bp double-strand DNA oligonucleotides encompassing the 19-nucleotide interfering sequence 5′-GCCAGAAGACCATGGATGA-3′ and a hairpin-forming sequence, which were cloned in these plasmids. Equivalent sequences 5′-ACACAAGACCACAGATGAT-3′ (mouse DGKα) or 5′-CTATGT GACTGAGATCGCA-3′ (human DGKζ) for DGK isoforms were used in negative-control plasmids. For transfection experiments, cells were transiently transfected with 20–30 μg of the plasmids as described.[32] Expression vectors for DGKs or siRNAs vectors were co-transfected in Jurkat cells in molar excess (3 : 1) to exosome reporters (GFP-CD63).

Isolation of exosomes. The exosomes produced by equal number of cells for each experimental condition were isolated from the cell-culture supernatants as previously described.[6,7] Using these standard protocols, culture supernatants of 20×10^6 cells were centrifuged at low speed in sequential steps, and then clarified to eliminate cells and cell debris. To obtain the exosomes from cells expressing the exosome reporters GFP-CD81, GFP-CD63 and DsRed2-CD63, a similar protocol

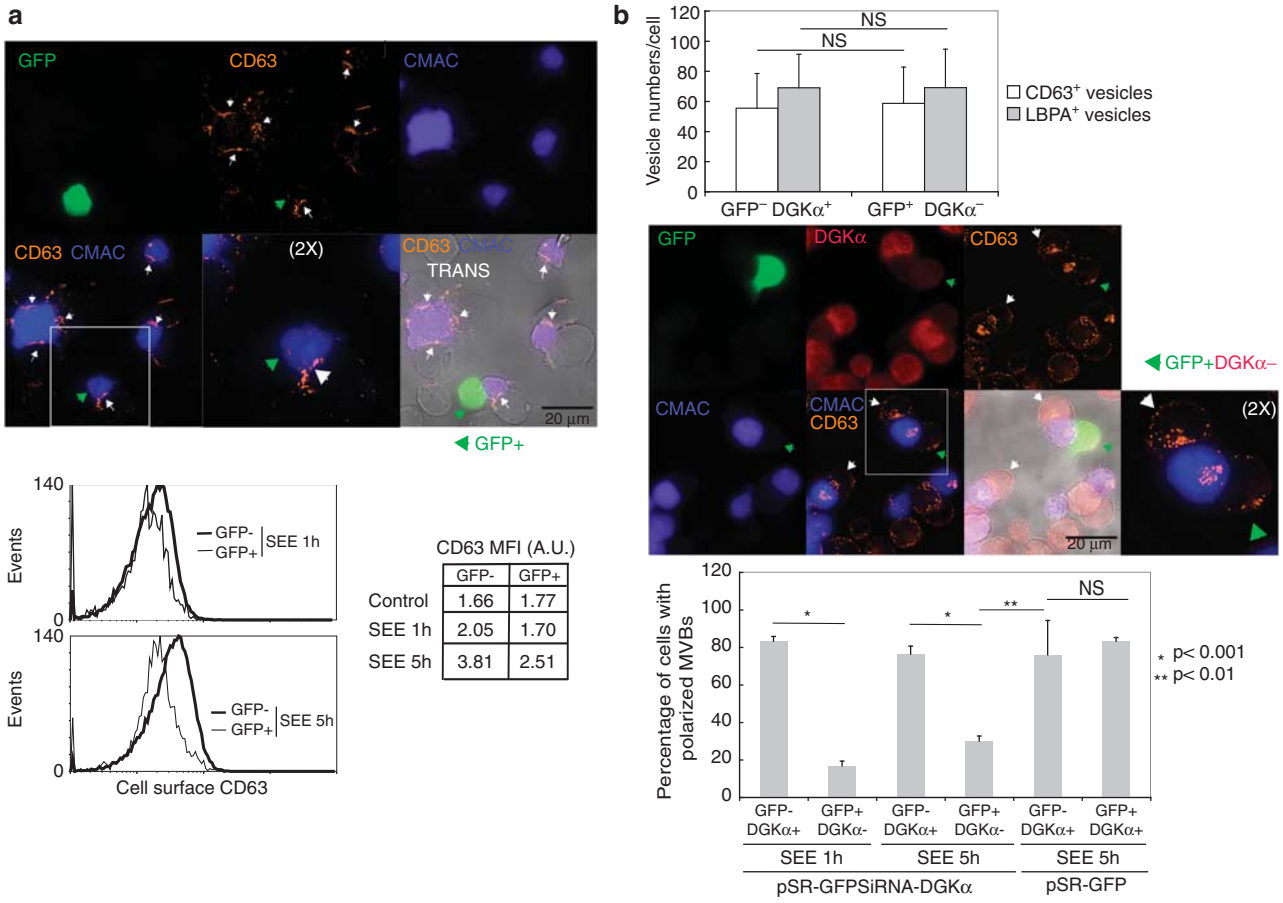

Figure 9 Interference of DGKα affects polarisation and degranulation of MVBs at the immune synapse. Jurkat cells transfected with a GFP-containing, bicistronic interference plasmid for human DGKα were stimulated for 1 and 5 h with Raji cells previously pulsed with SEE and labelled with CMAC (blue), to induce synapse formation and the polarised traffic of MVBs. (**a**) Upper panel: Degranulation of MVBs at the synapse after 5 h was assessed by cell surface staining of endogenous CD63 (orange-red) and fluorescence microscopy. White arrowheads label the synaptic contact areas made by GFP^- Jurkat cells, whereas green arrowhead labels the synapse corresponding to a GFP^+ Jurkat cell. Images are representative of the results obtained in four different experiments. Lower panel: degranulation induced by SEE was measured after 1 and 5 h, by analysing cell surface staining of CD63 in both GFP^+ ($DGK\alpha^-$) and GFP^- ($DGK\alpha^+$) Jurkat cells by flow cytometry. The FACS profiles corresponding to the staining of Jurkat cells challenged with Raji without SEE are not shown for clarity, but the corresponding mean fluorescence intensity data are included (control). (**b**) Upper panel: quantification of $LBPA^+$ and $CD63^+$ intracellular vesicles in Jurkat cells forming synapse with SEE-pulsed Raji cells during 5 h. Middle panel: polarisation of MVBs towards the synapse after 5 h was assessed by intracellular labelling of endogenous CD63 (orange-red). Interference with DGKα expression was tested by intracellular staining of endogenous DGKα (red). White arrowheads label synapses made by GFP^- $DGK\alpha^+$ Jurkat cells, whereas green arrowhead labels the synapse corresponding to a GFP^+ $DGK\alpha^-$ Jurkat cell. Images are representative of the results obtained in four different experiments. The inset shows a $\times 2$ digital zoom of the indicated areas. Lower panel: the graph summarises the results of four independent experiments (at least 40 cells per condition were analysed) similar to the one described in the middle panel, and compares the percentage of cells with polarised MVBs after 1 and 5 h of stimulation, both in $DGK\alpha^+$ cells and in $DGK\alpha^-$ cells. Cells with polarised MVBs were defined as those cells on which the majority of their MVBs were located at a distance of the synapse lower than one quarter of the diameter of the cell. The interference on DGKα expression does not affect the interaction among T lymphocytes and the SEE-presenting cells, as the frequency of formation of Raji/Jurkat conjugates was not affected by DGKα interference (not shown)

was performed, although 1×10^6 effector cells (Jurkat) were used. For the secretion of exosomes in immune synapse experiments, expression vectors for DGKs or siRNAs vectors were co-transfected in Jurkat cells in molar excess (3 : 1) to exosome reporter vectors (i.e., GFP-CD63), and the formation of synapses with Raji cells in the absence (control) or presence of superantigen (SEE) was performed at 2–3 days after transfection, as described below. The exosomes were recovered by ultracentrifugation ($100\,000 \times g$ for 12 h) as described,[6] and resuspended in 50 μl of RIPA lysis buffer, or directly quantified by flow cytometry (see below). We usually loaded 25 μl of this lysate per lane for WB analysis. We commonly obtained between 50–150 μg of protein in the $100\,000 \times g$ pellet from 20×10^6 CCh-stimulated cells. In the experiments that involved the isolation of exosomes and WB, each lane of the blot contained the total protein that was recovered in the culture medium from the same number of cells, untreated or treated with stimuli in the presence or in the absence of DGK inhibitor. The lysates of the cells recovered after the first step of the protocol for exosome isolation were run in parallel to the exosomes, to internally normalise WBs by viable cell number at the end of the culture period for exosome secretion, but also to normalise transfection efficiency of the XFP-CD63 reporter. Alternatively, the number of exosomes in the clarified culture supernatants was quantified by flow cytometry, using a constant acquisition period (5 min) and calibration fluorescent beads (50 and 100 nm beads, from Sigma). Forward- and side-scatter light detectors, together with gating regions, were set up to detect properly the calibration beads, and the absolute number of gated events equal to the number of exosomes was represented using dot plot (forward *versus* side-scatter) analysis. In parallel, samples corresponding to complete medium including the different reagents, but in the absence of cells, were analysed, and these dot plots registered a constant number of events; thus events above this background were considered as specific, cell-produced vesicles.

Western blot analysis. Cells and exosomes were lysed for 10 min in RIPA buffer containing protease inhibitors, and the proteins were separated by SDS-PAGE under reducing conditions and transferred to Hybond ECL membranes (GE Healthcare, Piscataway, NJ, USA). For CD63 detection, proteins were separated under non-reducing conditions as described.[8] After incubation with the appropriate primary antibody, the blots were developed with horseradish peroxidase-conjugated secondary antibodies using enhanced chemiluminescence reagents and following standard protocols.

Cell fractionation. J-HM1-2.2 cells were disrupted in 2 ml of an iso-osmotic homogenisation buffer[2] and the homogenate was fractionated on a discontinuous Percoll (Amersham Pharmacia) gradient as described.[2,8] The subcellular fractions, from the same number of control and stimulated cells, were analysed in parallel for the presence of CD63, FasL, DGKα and Lamp-1 proteins by WB. Lamp-1 was used as an appropriate, internal loading control. Density was calibrated using density marker beads (Amersham Pharmacia).

Electron microscopy. JHM1-2.2 cells were fixed for 20 min at RT in 2% PFA/1.5% glutaraldehyde in 0.1 M sodium cacodylate, pH 7.4. Cells were washed twice in 0.1 M sodium cacodylate and were spun into a tight pellet for osmication with 1.5% potassium ferricyanide, 1% osmium for 1 h at 4 °C. The cell pellet was washed several times with 0.1 M sodium cacodylate and incubated with 1% tannic acid in 0.05 M sodium cacodylate for 45 min at room temperature. The cell pellet was rinsed in 1% sodium sulphate in 0.05 M sodium cacodylate for 5 min and with dH_2O for 3 min. The cell pellet was dehydrated stepwise in ethanol (70–90% absolute ethanol). Ethanol was removed and propylene oxide was added for 2×10 min, and the cell pellet was embedded in 1 : 1 mixture of epon and propylene oxide. Ultrathin sections (60–70 nm) were cut on an ultramicrotome, collected onto grids and examined with a Philips EM420 transmission electron microscope (Hillsboro, OR, USA).

Immunofluorescence analysis. For fluorescence analysis of living J-HM1-2.2 cells expressing the different constructions, cells were attached to glass bottom 35 mm culture dishes (Mat-Tek, Ashland, MA, USA) using fibronectin at 24–48 h post transfection, and stimulated in culture medium without phenol red at 37 °C.[32] In some experiments, immune synapses between GFP-CD63-expressing Jurkat cells and Raji B cells, pulsed with superantigen SEE and labelled with CMAC, were performed as previously described.[24] Subsequently, epifluorescence images were taken with a Nikon Eclipse (Melville, NY, USA) TE2000S microscope equipped with a DS-5M digital camera and a Plan Apo VC $\times$ 60 NA 1.4 objective. Time-lapse analysis was performed in living cells using ACT2-U software or NIS-AR software (NIKON). After the culture period, samples were either cell-surface stained or fixed and stained as described[32] with primary Abs (anti-CD63, anti-LBPA, anti-DGKα and anti-FasL) and appropriate secondary Alexa Fluor-conjugated abs (Invitrogen). Confocal microscopy was performed using a Bio-Rad (Hercules, CA, USA) Radiance 2100 scan head mounted on a Nikon ECLIPSE TE 2000U microscope and using $\times$ 60 NA 1.4 PlanApo objective. No labelling was observed when using the secondary abs alone. The *z* axis projection (maximum intensity) and merged images for colocalisation experiments were performed using ImageJ software (Rasband, W.S., ImageJ, National Institutes of Health, Bethesda, MD, USA, http://rsb.info.nih.gov/ij/, 1997–2004). For quantification, digital images were analysed using EasiVision SIS image analysis software (Soft Imaging Software, Munster, Germany) and ImageJ software. Experimental significance of the results obtained at the single-cell level was achieved by analysing a minimal number of 60 cells (unless otherwise indicated) from different microscope fields, and a minimal number of three independent experiments. Results were expressed as average minus/plus standard deviation (S.D.), and correspond to the means of the separate experiments, and not to the pooled cells measured together. ANOVA analysis was performed for statistical significance of all the results. Trajectories of vesicles in videos were plotted by using NIS-AR software (NIKON). Epifluorescence image improvement was achieved by using deconvolution software (Huygens, Hilversum, The Netherlands, SVI).

Flow cytometry. After the indicated culture periods, cells were fixed and intracellularly stained with no Abs (negative controls) or primary Abs (anti-CD63, anti-LBPA and anti-FasL) and appropriate secondary, PE or FITC-conjugated Abs (Becton Dickinson, San Jose, CA, USA). A minimal number of 10 000 cells were analysed for FL-1 or FL-2 fluorescence by using FACSCAN flow cytometer (Becton Dickinson). For the experiments involving analysis of cell surface CD63 on Jurkat cells after synapse formation, Raji cells preloaded with CMAC were excluded from the flow cytometry analysis by electronic gating of CMAC-negative cells, and comparison of the CD63 red fluorescence on both Jurkat GFP^- and GFP^+ cells was performed using a FACS-Vantage flow cytometer equipped with an UV excitation laser (San Jose, CA, USA).

Conflict of interest

The authors declare no conflict of interest.

Acknowledgements. We thank Dr. G Griffiths (University of Oxford, UK), Dr. P Whitley (University of Bath, UK), and Dr. Sanchez-Madrid (Hospital de la Princesa, Madrid, Spain) for generously providing us some of the plasmids used in this study. We thank Alba Garcia and Ana Sanchez for their excellent technical support. This work was supported by grants from the Ministerio de Ciencia e Innovación, BFU2007-61613 and BFU2010-18726. R Alonso was the recipient of a fellowship from the Spanish Ministerio de Ciencia y Tecnología. A Fraile-Ramos is supported by the Ramón y Cajal Program. M Marsh is supported by the UK Medical Research Council. A Avila-Flores was supported by an AECC fellowship.

1. Stoorvogel W, Kleijmeer MJ, Geuze HJ, Raposo G. The biogenesis and functions of exosomes. *Traffic* 2002; **3**: 321–330.
2. Bossi G, Griffiths GM. Degranulation plays an essential part in regulating cell surface expression of Fas ligand in T cells and natural killer cells. *Nat Med* 1999; **5**: 90–96.
3. Nagata S. Apoptosis by death factor. *Cell* 1997; **88**: 355–365.
4. Zuccato E, Blott EJ, Holt O, Sigismund S, Shaw M, Bossi G *et al.* Sorting of Fas ligand to secretory lysosomes is regulated by mono-ubiquitylation and phosphorylation. *J Cell Sci* 2007; **120**: 191–199.
5. Monleon I, Martinez-Lorenzo MJ, Monteagudo L, Lasierra P, Taules M, Iturralde M *et al.* Differential secretion of Fas ligand- or APO2 ligand/TNF-related apoptosis-inducing ligand-carrying microvesicles during activation-induced death of human T cells. *J Immunol* 2001; **167**: 6736–6744.
6. Martinez-Lorenzo MJ, Anel A, Gamen S, Monleon I, Lasierra P, Larrad L *et al.* Activated human T cells release bioactive Fas ligand and APO2 ligand in microvesicles. *J Immunol* 1999; **163**: 1274–1281.
7. Andreola G, Rivoltini L, Castelli C, Huber V, Perego P, Deho P *et al.* Induction of lymphocyte apoptosis by tumor cell secretion of FasL-bearing microvesicles. *J Exp Med* 2002; **l95**: 1303–1316.
8. Alonso R, Rodriguez MC, Pindado J, Merino E, Merida I, Izquierdo M. Diacylglycerol kinase alpha regulates the secretion of lethal exosomes bearing Fas ligand during activation-induced cell death of T lymphocytes. *J Biol Chem* 2005; **280**: 28439–28450.
9. Kayagaki N, Kawasaki A, Ebata T, Ohmoto H, Ikeda S, Inoue S *et al.* Metalloproteinase-mediated release of human Fas ligand. *J Exp Med* 1995; **182**: 1777–1783.
10. Topham MK, Prescott SM. Mammalian diacylglycerol kinases, a family of lipid kinases with signaling functions. *J Biol Chem* 1999; **274**: 11447–11450.
11. Sanjuan MA, Jones DR, Izquierdo M, Merida I. Role of diacylglycerol kinase alpha in the attenuation of receptor signaling. *J Cell Biol* 2001; **153**: 207–220.
12. Strasser A. Death of a T cell. *Nature* 1995; **373**: 385–386.
13. Izquierdo M, Ruiz-Ruiz MC, Lopez-Rivas A. Stimulation of the Ptdlns turnover is a key event for Fas-dependent, activation-induced apoptosis in human T lymphocytes. *J Immunol* 1996; **157**: 21–28.
14. Roth MG. Lipid regulators of membrane traffic through the golgi complex. *Trends Cell Biol* 1999; **9**: 174–179.
15. Baron CL, Malhotra V. Role of diacylglycerol in PKD recruitment to the TGN and protein transport to the plasma membrane. *Science* 2002; **295**: 325–328.
16. Sprong H, van der Sluijs P, van Meer G. How proteins move lipids and lipids move proteins. *Nat Rev Mol Cell Biol* 2001; **2**: 504–513.
17. Quann EJ, Merino E, Furuta T, Huse M. Localized diacylglycerol drives the polarization of the microtubule-organizing center in T cells. *Nat Immunol* 2009; **10**: 627–635.
18. Vanlandingham PA, Ceresa BP. Rab7 regulates late endocytic trafficking downstream of multivesicular body biogenesis and cargo sequestration. *J Biol Chem* 2009; **284**: 12110–12124.
19. Clark RH, Stinchcombe JC, Day A, Blott E, Booth S, Bossi G *et al.* Adaptor protein 3-dependent microtubule-mediated movement of lytic granules to the immunological synapse. *Nat Immunol* 2003; **4**: 1111–1120.
20. Alonso R, Mazzeo C, Merida I, Izquierdo M. A new role of diacylglycerol kinase alpha on the secretion of lethal exosomes bearing Fas ligand during activation- induced cell death of T lymphocytes. *Biochimie* 2007; **89**: 213–221.
21. Jiang Y, Sakane F, Kanoh H, Walsh JP. Selectivity of the diacylglycerol kinase inhibitor 3-[2-(4-[bis-(4-fluorophenyl)methylene]-l-piperidinyl)ethyl]-2, 3-dihydro-2-thioxo-4(1H)quinazolinone (R59949) among diacylglycerol kinase subtypes. *Biochem Pharmacol* 2000; **59**: 763–772.
22. Bishop N, Woodman P. ATPase-defective mammalian VPS4 localizes to aberrant endosomes and impairs cholesterol trafficking. *Mol Biol Cell* 2000; **11**: 227–239.

23. Fujita H, Yamanaka M, Imamura K, Tanaka Y, Nara A, Yoshimori T *et al.* A dominant negative form of the AAA ATPase SKD1/VPS4 impairs membrane trafficking out of endosomal/lysosomal compartments: class E vps phenotype in mammalian cells. *J Cell Sci* 2003; **116**: 401–414.
24. Montoya MC, Sancho D, Bonello G, Collette Y, Langlet C, He HT *et al.* Role of ICAM-3 in the initial interaction of T lymphocytes and APCs. *Nat Immunol* 2002; **3**: 159–168.
25. Sato M, Ueda Y, Umezawa Y. Imaging diacylglycerol dynamics at organelle membranes. *Nat Methods* 2006; **3**: 797–799.
26. Matsuo H, Chevallier J, Mayran N, Le Blanc I, Ferguson C, Faure J *et al.* Role of LBPA and Alix in multivesicular liposome formation and endosome organization. *Science* 2004; **303**: 531–534.
27. Kobayashi T, Beuchat MH, Chevallier J, Makino A, Mayran N, Escola JM *et al.* Separation and characterization of late endosomal membrane domains. *J Biol Chem* 2002; **277**: 32157–32164.
28. Carrasco S, Merida I. Diacylglycerol-dependent binding recruits PKC(theta) and RasGRPI Cl domains to specific subcellular localizations in living T lymphocytes. *Mol Biol Cell* 2004; **15**: 2932–2942.
29. Desai DM, Newton ME, Kadlecek T, Weiss A. Stimulation of the phosphatidylinositol pathway can induce T cell activation. *Nature* 1990; **348**: 66–69.
30. Santos T, Carrasco S, Jones DR, Merida I, Eguinoa A. Dynamics of diacylglycerol kinase zeta translocation in living T-cells. Study of the structural domain requirements for translocation and activity. *J Biol Chem* 2002; **277**: 30300–30309.
31. Whitley P, Reaves BJ, Hashimoto M, Riley AM, Potter BV, Holman GD. Identification of mammalian Vps24p as an effector of phosphatidylinositol 3,5-bisphosphate-dependent endosome compartmentalization. *J Biol Chem* 2003; **278**: 38786–38795.
32. Jambrina E, Alonso R, Alcalde M, Rodríguez MC, Serrano A, Martínez-AC *et al.* Calcium influx through receptor-operated channel induces mitochondria-triggered paraptotic cell death. *J Biol Chem* 2003; **278**: 14134–14145.
33. Kobayashi T, Stang E, Fang KS, de Moerloose P, Parton RG, Gruenberg J. A lipid associated with the antiphospholipid syndrome regulates endosome structure and function. *Nature* 1998; **392**: 193–197.
34. Babst M. A protein's final ESCRT. *Traffic* 2005; **6**: 2–9.
35. Babst M, Wendland B, Estepa EJ, Emr SD. The Vps4p AAA ATPase regulates membrane association of a Vps protein complex required for normal endosome function. *EMBO J* 1998; **17**: 2982–2993.

Supplementary Information accompanies the paper on Cell Death and Differentiation website (http://www.nature.com/cdd)